An Omnidirectional Dual-Reflector Antenna with a Shaped Main Reflector Described by Local Conic Sections

Rafael A. Penchel*, José R. Bergmann*, and Fernando J. S. Moreira+

*CETUC, PUC-Rio, Rua Marques de São Vicente 225, 22453-900, Rio de Janeiro, Brazil

{rapenchel, bergmann}@.cetuc.puc-rio.br

+DELT, UFMG, Av. Antônio Carlos 6627, 31270-901, Belo Horizonte, MG, Brazil

fernandomoreira@ufmg.br

***Abstract*— This work investigates the synthesis of dual-reflector antennas for omnidirectional coverage. Both reflectors are bodies-of-revolution: the subreflector is generated by a single conic section while the shaped main reflector is generated by a series of local conic sections which are consecutively concatenated. The main-reflector is shaped to radiate, under GO principles, a prescribed power density in the elevation plane. To illustrate the method, two representative omnidirectional axis-displaced Cassegrain configurations are synthesized. The GO shaping results are validated by method-of-moments simulations.**

I. INTRODUCTION

The growing demand for broadband Internet access as well as the increasing quality and speed of communication links have set an important niche market known as "last mile" access. WiMax systems, which are based on the cellular concept, may be employed in these services. Furthermore, by operating in the microwave and millimetre-wave ranges, one may employ reflector antennas while planning cells with omnidirectional coverage. The main advantages of this kind of antennas are their potentially high gain and relatively broad operation band.

Omnidirectional dual-reflector antennas with a shaped main reflector may be synthesized to provide a prescribed radiation pattern in the elevation plane [1]. Some reflector shaping techniques are based on the numerical integration of an ordinary differential equation derived from Geometrical Optics (GO) principles [1]. Recently, a technique based on the combination of local conic sections has been presented for the shaping of Cassegrain and Gregorian antennas [2]. The formulation was improved [3] and then extended to the shaping of omnidirectional dual-reflector configurations [4]. In [2]-[4], both sub- and main-reflectors are shaped to provide a uniform phase distribution at the main-reflector aperture. In the present work, we extend the concepts of [2]-[4] to the design of omnidirectional dual-reflector antennas where only the main reflector is shaped to provide the desired radiation pattern in the elevation plane. To illustrate the proposed technique, a design similar to that presented in [5] is investigated. It is shown that the present shaping technique converges much more rapidly than the technique based on the numerical integration of a differential equation [1].

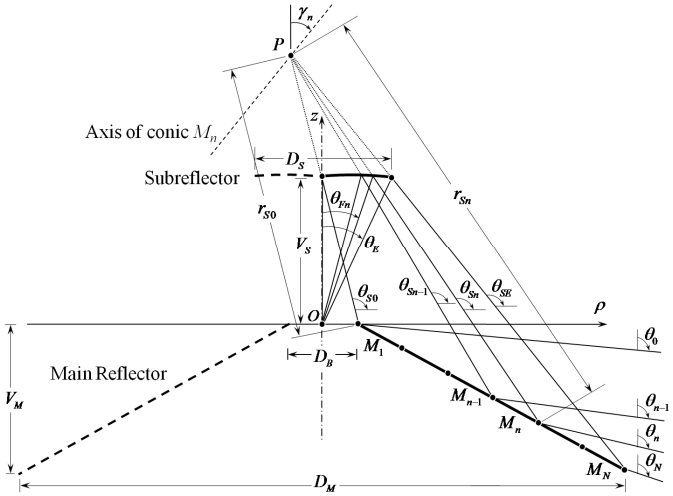

Fig. 1 - Conic sections representing the generatrix shaped main reflector

II. MAIN-REFLECTOR SHAPING TECHNIQUE

In the present shaping technique, the axis-symmetric subreflector is generated by a conic section, while the main reflector is generated by the consecutive combination of local conic sections. A procedure for the definition of the subreflector conic generatrix is discussed in [1]. This conic has 2 focci: one located at the origin (O), where the feed phase center is supposed to be, and another at P, which defines the subreflector annular caustic (see Fig. 1). As the subreflector generating conic is known, the relation between the feed-ray direction (θ_F) and the direction of the ray reflected by the subreflector (θ_S) is also known [1]. The main reflector is generated by several local conic section M_n ($n = 1, \ldots, N$), all of them with one of their focci at P. The axis of M_n passes through P and makes an angle γ_n with the z-direction (Fig. 1). In order to uniquely define the main-reflector local conic sections, three parameters must be determined for each M_n: the inter-focal distance ($2c_n$), the eccentricity (e_n), and the tilt

with the help of the following auxiliary parameters [6]:

$$a_n = c_n\left(e_n - 1/e_n\right) \tag{1}$$

$$b_n = e_n \sin\gamma_n \tag{2}$$

$$d_n = e_n \cos\gamma_n - 1 \tag{3}$$

Three equations are needed to obtain the parameters a_n, b_n, and d_n at each step n of the iterative process. From the polar equation of M_n, the distance from P to M_n is given by:

$$r_S = \frac{a_n}{b_n \sin\theta_S + (1+d_n)\cos\theta_S - 1}, \quad \text{for } \theta_{Sn-1} \le \theta_S \le \theta_{Sn} \tag{4}$$

Since θ_{Sn-1} and r_{Sn-1} are both known from the previous step (n–1), from (4) one obtains:

$$r_{Sn-1} = \frac{a_n}{b_n \sin\theta_{Sn-1} + (1+d_n)\cos\theta_{Sn-1} - 1} \tag{5}$$

Also from the polar equation of M_n one obtains that

$$b_n\left[\cot\left(\frac{\theta}{2}\right) + \cot\left(\frac{\theta_S}{2}\right)\right] + d_n\left[\cot\left(\frac{\theta}{2}\right)\cot\left(\frac{\theta_S}{2}\right) - 1\right] = 2, \tag{6}$$

for $\theta_{Sn-1} \le \theta_S \le \theta_{Sn}$ and $\theta_{n-1} \le \theta \le \theta_n$, where θ is the direction of the ray reflected by the main reflector (Fig. 1). As θ_{Sn-1} and θ_{n-1} are known from the previous step, from (6) one obtains:

$$b_n\left[\cot\left(\frac{\theta_{n-1}}{2}\right) + \cot\left(\frac{\theta_{Sn-1}}{2}\right)\right] + d_n\left[\cot\left(\frac{\theta_{n-1}}{2}\right)\cot\left(\frac{\theta_{Sn-1}}{2}\right) - 1\right] = 2 \tag{7}$$

Finally, the conservation of energy along the tube of rays departing from O toward the main-reflector far-field region is imposed:

$$\int_0^{\theta_{Fn}} G_F(\theta_F)\sin\theta_F \, \mathrm{d}\theta_F = N_F \int_{\theta_0}^{\theta_n} G_A(\theta)\sin\theta \, \mathrm{d}\theta \tag{8}$$

where $G_F(\theta_F)$ and $G_A(\theta)$ are the circularly-symmetric radiation patterns of the feed and the antenna, respectively, θ_0 is the prescribed direction of the ray reflected by the main reflector corresponding to the feed principal ray ($\theta_F = 0$), and N_F is a normalization constant give by

$$N_F = \int_0^{\theta_E} G_F(\theta_F)\sin\theta_F \, \mathrm{d}\theta_F \Big/ \int_{\theta_0}^{\theta_N} G_A(\theta)\sin\theta \, \mathrm{d}\theta \tag{9}$$

where θ_0 and θ_N are the far field limits under GO principles. If $\theta_0 > \theta_N$ the structure of rays corresponds to a main reflector with real caustic. If $\theta_N > \theta_0$, then the caustic is virtual. Once θ_n is numerically determined from (8), the third shaping equation is obtained from (6):

$$b_n\left[\cot\left(\frac{\theta_n}{2}\right) + \cot\left(\frac{\theta_{Sn}}{2}\right)\right] + d_n\left[\cot\left(\frac{\theta_n}{2}\right)\cot\left(\frac{\theta_{Sn}}{2}\right) - 1\right] = 2 \tag{10}$$

From (5), (7), and (9) a set of three linear equations are established to determine a_n, b_n, d_n, and, with the help of (1)-(3), $2c_n$, e_n, γ_n.

The iterative process starts at $n = 0$, with $\theta_{F0} = 0$ (θ_{S0} is obtained from θ_{F0} with the help of the subreflector conic equation), $\theta = \theta_0$, and r_{S0} given by the location of the subreflector caustic P and by the desired diameter D_B of the main-reflector central opening (see Fig. 1).

III. Case Studies

To illustrate the shaping procedure described in the previous section, two case studies are discussed: the first example is designed to provide a sectoral coverage in the elevation plane over ±7.5° with respect to the horizon, while the second provides a sectoral coverage over ±15°. In both examples the antennas have been scaled to have a conical projected aperture width (W_A) equal to 8.25λ or 16.5λ.

The feed is assumed to be a TEM coaxial horn. The function that describes the radiation pattern of the feeder in the far-field region is given by [1]:

$$G_F(\theta_F) = G_{0F}\left[\frac{J_0(kr_i\sin\theta_F) - J_0(kr_e\sin\theta_F)}{\sin\theta_F}\right]^2 \tag{11}$$

where G_{0F} is a normalization factor, r_i and r_e are the internal and external radii, respectively. In all case studies to be presented, $r_i = 0.45\lambda$ and $r_e = 0.90\lambda$. The objective function that describes the sectoral radiation pattern of the dual-reflector antenna in the elevation plane is given by

$$G_A(\theta) = \frac{1}{2\pi}\left|\frac{1}{\cos\theta_1 - \cos\theta_2}\right| \tag{12}$$

which has been normalized for unit radiated power.

A. *OADC Configuration for Sectoral Coverage over ±7.5°*

In the first case study (Case A.I), the main reflector of an omnidirectional axis-displaced Cassegrain (OADC) configuration was synthesized to radiate, under GO principles, a sectoral illumination in the elevation plane over ±7.5° with respect to the horizon (i.e., from $\theta = \theta_N = 82.5°$ to $\theta = \theta_0 = 97.5°$). As $\theta_0 > \theta_N$, the main reflector has a real caustic (see Fig. 2). This is basically the design presented in [5], except that here the feed is simulated as a TEM coaxial horn and the subreflector is generated by an ellipse to avoid rays being reflected back to the feed aperture. That can be noticed from Fig. 2 by observing the direction of the rays reflected by subrefletor. By minimizing the scattering back to the feed aperture one may end up improving the return-loss behaviour across the operation bandwidth (such topic is beyond the objectives of the present work).

The subreflector generating ellipse was determined from a classical OADC configuration with the following parameters [1] (some of them are illustrated in Fig. 1): $V_S = 9.5\lambda$, $D_B = 2.4\lambda$, main-reflector projected diameter $D_M = 20\lambda$, focus O at the plane of the main-reflector central opening ($z_B = 0$), main-reflector aperture width $W_A = 8.25\lambda$, and $\gamma = 90°$. These values provide an ellipse with an eccentricity equal to 0.7871, an inter-focal distance equal to 69.93λ, and an axis with a tilt

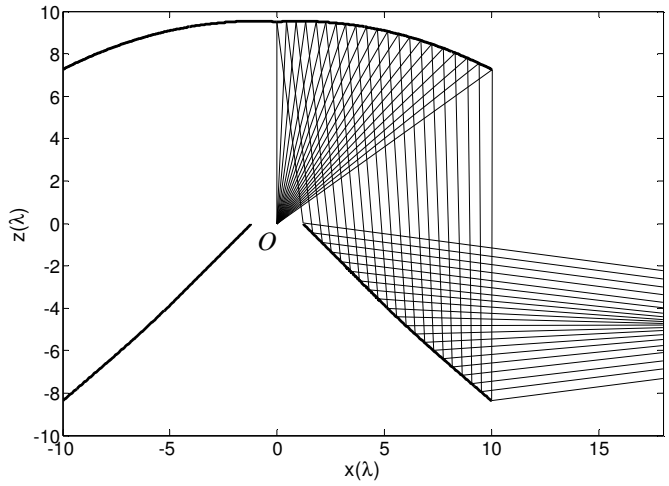

Fig. 2 – Generatrices of the shaped OADC dual-reflector antenna (Case A.I) with sectoral illumination in elevation plane over ±7.5° with respect to horizon.

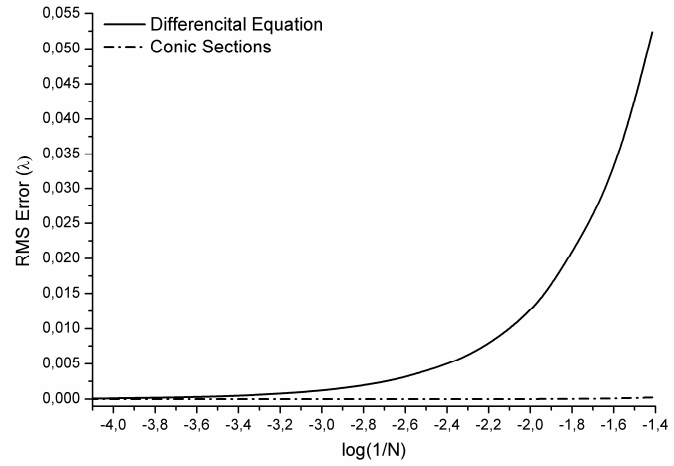

Fig. 3 – RMS error with respect to N of the main-reflector of Case A.I.

angle of 171.82° with respect to the z-axis. As a consequence, the projected diameter of the subreflector $D_S = 20.03\lambda$ and the subreflector edge angle $\theta_E = 54.07°$. These parameters also provide $r_{S0} = -69.77\lambda$ as an initial parameter for the shaping procedure presented in Sect. II. The negative value of r_{S0} indicates that the ring caustic P is *below* the main reflector (see Fig. 2). The generatrices of the subreflector and shaped main reflector are illustrated in Fig. 2.

The main-reflector shaping was also performed with the procedure described in [1], which is based on the numerical integration of a differential equation. The main-reflector RMS error (with respect to a reflector shaped with a very large N value) obtained by the present technique and that of [1] is depicted in Fig. 3 as a function of log(1/N), where N+1 is the total number of points over the main-reflector generatrix, obtained at each step of the shaping procedures (see Fig. 1). Only these N+1 points were considered in the RMS error calculation. The errors refer to r_S, i.e., the distance from P to the main reflector. From Fig. 3 one observes that, for this particular design, the present shaping procedure provides the same accuracy of the procedure presented in [1] using about 100 times less points.

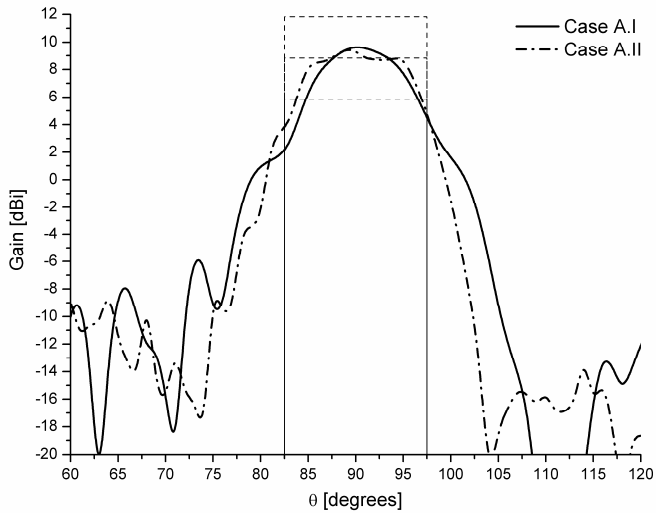

Fig. 4 – MoM radiation patterns (Cases A.I and A.II) in the elevation plane.

TABLE I

Parameters	Case A.I	Case A.II	Case B.I	Case B.II
W_A (λ)	8.25	16.50	8.25	16.50
V_S (λ)	9.50	19.00	9.50	19.00
D_M (λ)	20.00	40.00	20.00	40.00
D_B (λ)	2.40	4.80	2.40	4.80
D_S (λ)	20.03	40.06	20.03	40.06
V_M (λ)	8.37	16.74	8.58	17.16
e	0.787098	0.787098	0.787098	0.787098
θ_E	54.07°	54.07°	54.07°	54.07°

In another situation (Case A.II), the antenna of Case A.I was scaled to have its dimensions doubled. Its dimensions are listed in Table I. It is expected that contributions to the field generated by the diffraction phenomena and electromagnetic coupling are less significant and, consequently, the synthesis based on GO have a better result. The radiation patterns of Cases A.I and A.II were simulated by the method of moments (MoM) and are illustrated in Fig. 4, together with the prescribed GO far-field pattern of (8), used for the main-reflector shaping [7]. As expected, the antenna with a bigger aperture (Case A.II) presents a radiation pattern closer to the objective function than that of Case A.I.

B. OADC Configuration for Sectoral Coverage over ±15°

The omnidirectional ADC configuration of Case B.I was designed to radiate, once again, a sectoral illumination in the elevation plane but over a wider range (±15° with respect to the horizon, i.e., from $\theta = \theta_N = 75°$ to $\theta = \theta_0 = 105°$). The subreflector is the same of Case A.I and the main parameters are listed in Table I. The generatrices of the subreflector and shaped main reflector are illustrated in Fig. 5. The main-reflector RMS error of Case B.I is illustrated in Fig. 6 and

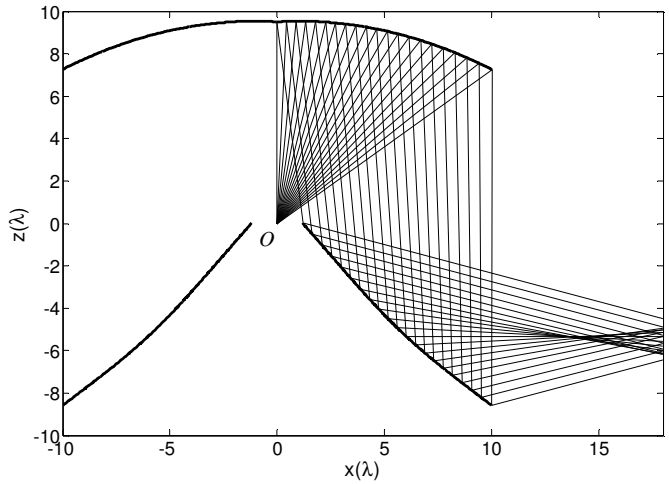

Fig. 5 – Generatrices of the shaped OADC dual-reflector antenna (Case B.I) with sectoral illumination in elevation plane over ±15° with respect to horizon.

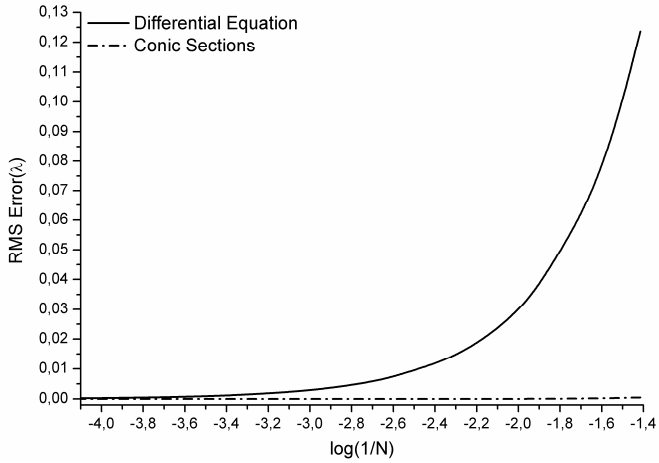

Fig. 6 – RMS error with respect to *N* of the main-reflector of Case B.I.

basically has the same behaviour of the RMS error of Case A.I (Fig. 3), differing only in the error scale.

In last situation analysed (Case B.II), the dual-reflector antenna of Case B.I was scaled to have its dimensions doubled (Table I). Figure 7 illustrates the MoM radiation patterns of Cases B.I and B.II, together with the prescribed GO pattern (8). One observes from Fig. 7 that the bigger antenna (Case B.II) provides a radiation pattern closer to the prescribed objective.

IV. Conclusions

This work presented a method for the GO synthesis of omnidirectional dual-reflector antennas. The procedure shapes the main-reflector generatrix, which is represented by local conic sections consecutively concatenated. The subreflector is not shaped and its generatrix is represented by a single conic section. Given the feed illumination, the main-reflector is shaped to radiate a prescribed power density in the elevation plane. The procedure was demonstrated in the synthesis of

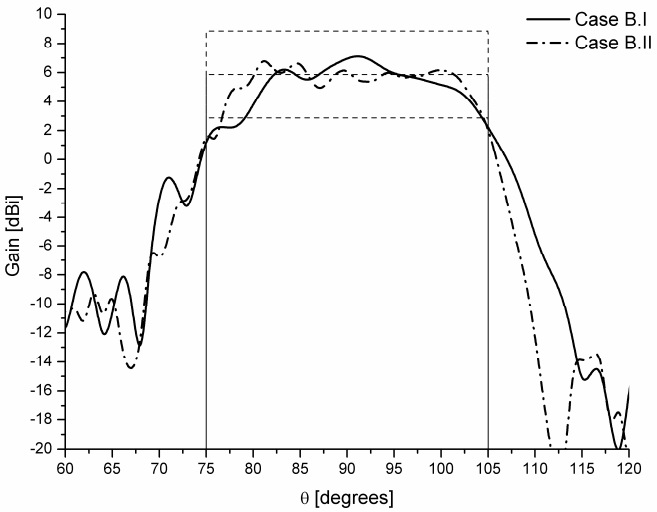

Fig. 7 – MoM radiation patterns (Cases B.I and B.II) in the elevation plane

two representative configurations, shaped to radiate a sectoral power density. For the case studies investigated here, the method has a numerical convergence higher than a traditional method based on the numerical integration of an ordinary differential equation.

Base on GO principles that shape the main reflector of omnidirectional dual-reflector antenna by concatenation of conic sections in other to obtain a uniform radiation pattern in elevation plane. Because this method does not solve any differential equation, it is numerically more efficient and converges faster than the traditional method. The formulation was applied to ADC-like configuration, but can be adapted to other axis displaced dual-reflector configuration.

Acknowledgment

This work was made possible by support from, MCT/FINEP/CT/CNPq-554661/2010-1, and INCT Wireless Communications CNPq-573939/2008-0.

References

[1] J. R. Bergmann and F. J. S. Moreira, "Omnidirectional ADE antenna with GO shaped main reflector for arbitrary far-field pattern in the elevation plane," IET Microwaves, Antennas & Propagation, vol. 3, no. 5, pp. 1028-1035, Oct. 2009.

[2] Y. Kim and T.-H. Lee, "Shaped circularly symmetric dual reflector antennas by combining local conventional dual reflector systems," IEEE Trans. Antennas Propagat. vol. 57, no 1, pp. 47-56, Jan. 2009.

[3] F. J. S. Moreira and J. R. Bergmann, "Shaping axis-symmetric dual-reflector antennas by combining conic sections," IEEE Trans. Antennas Propagat., accepted for publication.

[4] F. J. S. Moreira and J. R. Bergmann, "Omnidirectional dual-reflector shaping by concatenating conic sections," 4th European Conf. Antennas and Propagation (EuCAP 2010), Barcelona, Spain, April 2010.

[5] A. P. Norris and W. D. Waddoup, "A millimetric wave omnidirectional antenna with prescribed elevation shaping," in Proc. ICAP—4th Int. Conf. Antennas and Propagation, pp. 141-145, 1985.

[6] B. S. Westcott, F. A. Stevens, and F. Brickell, "GO synthesis of offset dual reflectors," IEE Proc., Pt. H, vol. 128, no. 1, pp. 11–18, Feb. 1981.

[7] J. R. Mautz and R. F. Harrington, "An Improved E-Field Solution for a Conducting Body of Revolution," Technical Report TR-80-1, Dept. Electrical and Computer Engineering, Syracuse University, 1980.